The Rate Acceleration in Solid-State Polycondensation of PET by Nanomaterials

Huimin Yu, Keqing Han, Muhuo Yu

State Key Laboratory of Chemical Fibers and Polymer Materials, College of Materials Science and Engineering, Donghua University, Shanghai 200051, People's Republic of China

Received 4 November 2003; accepted 2 April 2004
DOI 10.1002/app.20888
Published online in Wiley InterScience (www.interscience.wiley.com).

ABSTRACT: The effect of nanomaterials on the solid-state polycondensation (SSP) of PET was investigated using intrinsic viscosity measurement, wide-angle X-ray diffraction, differential scanning calorimetry, and polarizing microscope. The results showed that the montmorillonite nanomaterials could greatly increase the rate of solid-state polycondensation of PET, probably due to the nucleation of montmorillonite nanomaterials for PET crystallization, which resulted in lower crystallinity, more small crystals, and more surfaces of the crystals. The surfaces of microcrystal and richer amorphous regions benefitted the polycondensation reaction of PET and diffusion of volatile by-products, which led to the higher rate of SSP. © 2004 Wiley Periodicals, Inc. J Appl Polym Sci 94: 971–976, 2004

Key words: nanomaterials; montmorillonite; PET; solid-state polycondensation; crystallization

INTRODUCTION

PET/montmorillonite (MMT) nanocomposites have many great advantages compared with pure PET and have a large potential market in terms of engineering plastics, films, and packing bottles. PET is a commercially important polymer and is extensively used in the formation of staple and filament, fibers, films, bottles, plastic parts, etc. Commercial application of PET varies depending on its molecular weight. PET of molecular weight of 15,000 to 25,000 is used in textiles applications, whereas for injection or blow molding applications, PET with an average molecular weight greater than 30,000 is used.

For preparing PET, which has a molecular weight greater than 20,000, solid-state polycondensation (SSP) is generally preferred in industry. The SSP is carried out by heating the solid PET with low molecular weight below its melting point but well above its glass transition temperature. The process is carried out at approximately 200–240°C. Under these conditions, the polymer end-groups are sufficiently mobilized for a reaction to take place. The reaction by-products are removed by allowing a flow of inert gas or by maintaining reduced pressure. The main polycondensation reaction is an equilibrium reaction and the by-product, ethylene glycol (EG), is removed so that the forward reaction will be favored.

The polycondensation rate depends on both chemical and physical process, and the possible rate-determining steps are: (a) chemical reaction control, a reversible chemical reaction; (b) interior diffusion control, diffusion of the volatile reaction products in the solid polymer; and (c) surface diffusion control, diffusion of the volatile reaction products from the surface of the polymer to the inert gas.

Depending on the process and operating variables, the SSP rate is controlled by one or more of these steps. Much research is done to improve the rate of SSP [1–10]. The rate of polycondensation reaction and diffusion of volatile by-products in the SSP process should be related to the crystal structure; however, only a few articles[11] concerned the relations between the rate of SSP and crystallization. There are no published articles concerning the influence of nanomaterials on SSP. Therefore, the influence of nanomaterials on the SSP process of various polymers was investigated in our laboratory, and the influence of MMT nanomaterials on the SSP behavior of PET and the changes of PET crystalline structure in the SSP process were studied in this paper.

EXPERIMENTAL

Materials

The pure PET chips($[\eta]$ = 0.64) and PET/MMT chips with MMT mass proportion of 2.5% ($[\eta]$ =

Correspondence to: M. Yu (yumuhuo@dhu.edu.cn).

Journal of Applied Polymer Science, Vol. 94, 971–976 (2004)

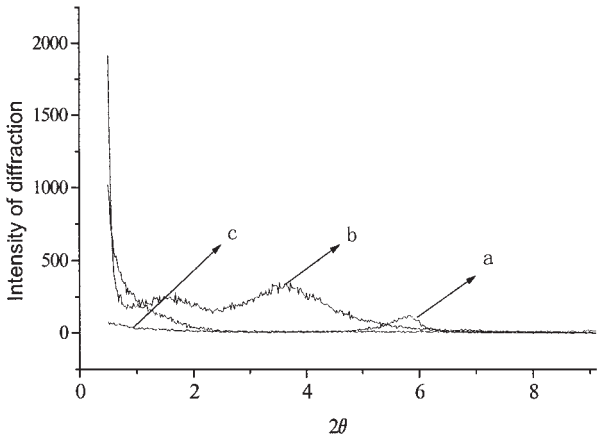

Figure 1 The WAXD patterns of PET/MMT (2.5%), Na-matrix MMT, and organophilic MMT: (a) Na-matrix MMT, (b) organophilic MMT, (c) PET/MMT (2.5%).

0.65) were produced by Yanshan Petrochemistry Inc. (China).

SSP and the intrinsic viscosity measurements

The SSP of pure PET and PET/MMT was carried out in a tumble reactor. Nitrogen gas was heated before it was passed through the tumble reactor and the nitrogen flow was controlled by a gas flow meter. The reactor was heated slowly to make the PET fully pre-crystallize until the temperature reached 230°C. Under these conditions, the SSP of PET and PET/MMT chips was carried out for 4, 7, 10, 15, 20, and 25 h.

The relative viscosity (η_r) of PET in tetrachloethane/phenol (1:1 by weight) at concentration (c = 0.5 g/dL) was determined using an Ubbelohde viscometer at 25°C. The intrinsic viscosity was calculated by the formula[12]

$$[\eta] = \frac{\sqrt{1 + 1.4\eta_{sp}} - 1}{0.7c}. \quad (1)$$

Wide-angle X-ray diffraction measurements (WAXD)

WAXD was carried out to test the changes of MMT interlayer spacing using a Model D/max 2550V automatic diffractometer in the reflection mode at 40 kV and 100 mA. The 2θ angle region range was between 0 and 10°.

To observe the crystal phenomenon of two samples after SSP of 20 h, WAXD was carried out using a Japanese Model D/max-B automatic diffractometer in the reflection mode at 40 kV and 40 mA with the Cu target and Ni wave filter. The 2θ angle region range was between 5 and 40°.

DSC measurements

To observe the effect of the MMT on the crystallization of PET, the DSC measurements were performed on a Perkin–Elmer Pyris1 differential scanning calorimeter in the nitrogen gas atmosphere. The nonisothermal crystallization of samples were studied under the following conditions: heated samples to 290°C at 10°C/min, kept for 5 min to avoid the thermal history, then cooled to 100°C at 160°C/min, finally heated to 290°C at 10°C/min.

To describe the crystallization and melting of samples with various SSP time, the differential scanning calorimetry data of samples were obtained with a Mettler Toledo System DSC 822^e differential scanning calorimeter in the nitrogen gas atmosphere. Samples were heated at 20°C/min to 290°C, maintained for 5 min to avoid the thermal history, then cooled to the room temperature at 10°C/min and finally heated to 290°C at 10°C/min.

Polarizing microscope observation

The crystalline form of PET and PET/MMT samples was observed using a Japanese Olympus BX51 polarizing microscope. Samples were heated to 290°C at

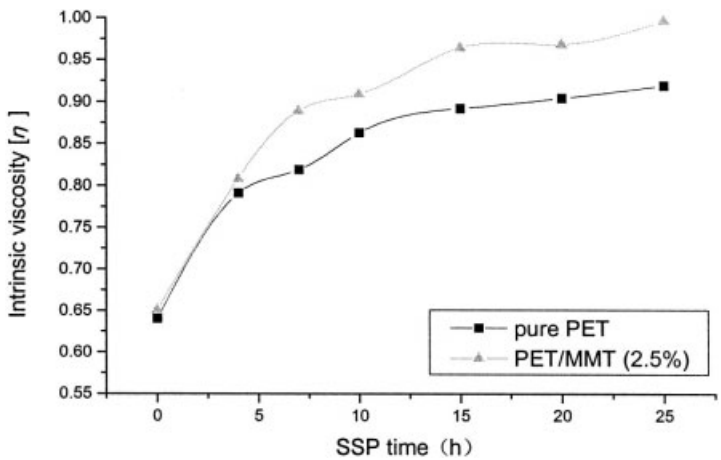

Figure 2 Relationship between intrinsic viscosity of PET and SSP time at 230°C.

TABLE I
Intrinsic Viscosity of Samples with Various SSP Times at 230°C 8

Time of SSP (h) samples	0	4	7	10	15	20	25
Pure PET	0.641	0.791	0.819	0.863	0.892	0.904	0.919
PET/MMT (2.5%)	0.651	0.808	0.889	0.909	0.964	0.968	0.996

100°C/min, kept for 3 min to make them fully melt, then cooled to 210°C at 130°C/min.

RESULTS AND DISCUSSION

Figure 1 shows the X-ray diffraction patterns of PET/MMT (2.5%), Na-matrix MMT, and organophilic MMT. As shown in Figure 1, there was an obvious diffraction peak on the Na-matrix MMT diffraction pattern near $2\theta = 5.8°$. According to Bragg's equation, the interlayer spacing of MMT d_{001} was 1.52 mm. The diffraction peak of the organophilic MMT WAXD pattern was near $2\theta = 3.6°$. So the interlayer spacing of MMT was obviously increased after being organically modified and the interior and exterior surfaces were changed from hydrophilicity to organophobicity, which reduced the surface energy of silicate layers of MMT and promoted the formation of polymer/MMT nanocomposites since monomers or polymers entered the gap between MMT layers more easily. But there was no obvious diffraction peak on the PET/MMT(2.5%) WAXD pattern between $2\theta = 1°$ and $2\theta = 10°$. There were two possible reasons for the phenomenon: first, the content of the MMT in the composites was too low to see the rare weak diffraction peak; second, PET molecular chains have entered the MMT interlayer, the interlayer spacing has been increased, and the diffraction peak could be seen only when $2\theta < 1°$. So we draw a conclusion from the latter reason that the MMT layers in PET/MMT have been exfoliated.

The intrinsic viscosity of both pure PET and PET/MMT with various SSP times was plotted, as shown in Figure 2 and Table I. The SSP rate acceleration by the MMT nanomaterials can be clearly seen in Figure 2. For example, the intrinsic viscosity of PET/MMT with 8 h SSP was almost equal to that of the pure PET with 15 h SSP. The SSP rate nearly doubled. This SSP rate enhancement would be very useful for industrial production to improve the efficiency of SSP equipment and decrease the consumption of energy sources.

This SSP rate enhancement might be due to the catalysis of the nanomaterials on polycondensation, and we will carry out further investigations.

The enhancement might also be attributed to the fact that the gap between PET and MMT layers contributed to the diffusion of the volatile by-products (EG) in the solid polymer during the SSP process. In other words, the existence of the gap could change the equilibrium of the condensation reaction and further improve the ester exchange reaction to achieve higher molecular weight. On the other hand, the crystal dimension in the PET/MMT composites became much smaller than that of the pure PET, which formed many more surfaces of crystals, resulting from the nucleation of the MMT. These surfaces of crystals and interfaces between them would benefit the polycondensation of PET and the diffusion of the volatile by-products.

Many research papers [13–15] concerned the crystallization of PET and PET/MMT nanocomposites. According to the existing literature,[16] the effect of MMT on the crystalline performance is not well known yet. Most researchers considered that the nanoparticles of MMT dispersed in PET matrix acted as the nucleating agent in PET crystallization process. The strong interaction between PET and MMT restricted the motions of PET macromolecular segment and prohibited the growth of PET crystalline structure. Therefore, the

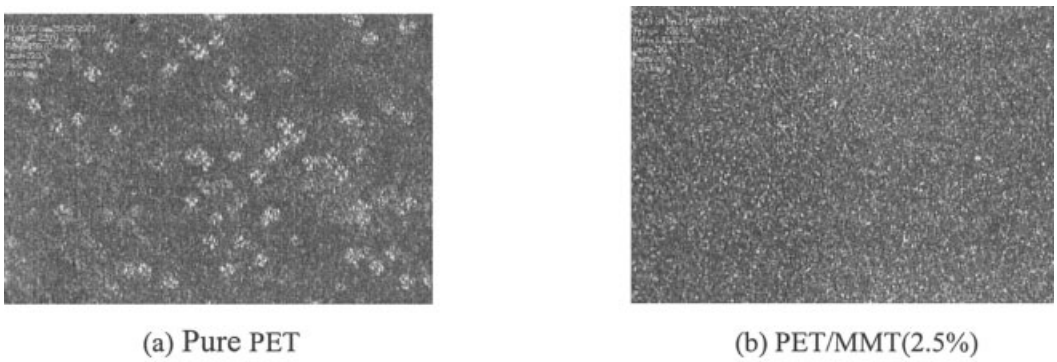

Figure 3 Polarizing microscope images of different PET samples.

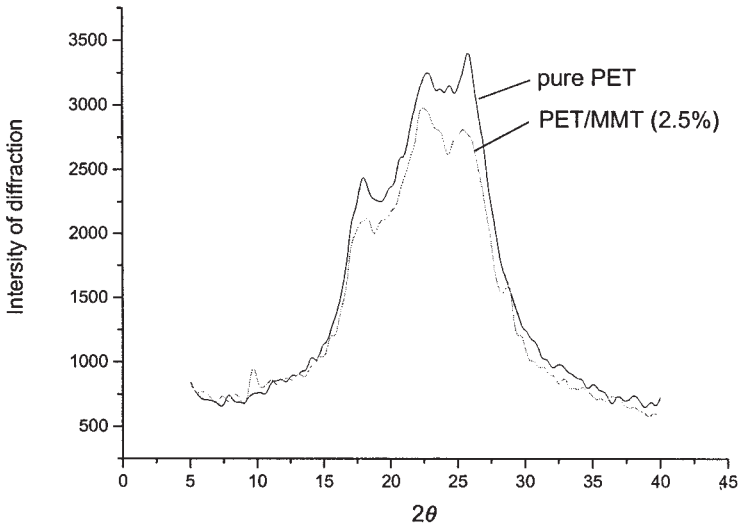

Figure 4 The WAXD patterns of pure PET and PET/MMT (2.5%) after 20 h SSP.

crystallization rate of PET depended on the synthetically actions from the two sides[17]. Some researchers also considered that neither quenching nor isothermal samples of PET/MMT showed perfect spherulite structure, while the crystallization rate of PET/MMT was increased for the nucleation[18].

Figure 3 shows the polarizing microscope images of the isothermal crystallization of pure PET and PET/MMT(2.5%) at 210°C. Figure 3a shows that many big spherulites in the process of isothermal crystallization form in pure PET, although the spherulite structure is not very perfect. Figure 3b shows that there is almost no spherulite but microcrystal in the PET/MMT nanocomposites. This phenomenon implied that the PET/MMT had difficulty forming a typical spherulite structure and only formed some microcrystals, which was in good agreement with the results of Guoyao[18]. This was attributed to the heterogeneous nucleation of MMT, which accelerated the speed of nucleation of PET and increased the number of the crystal nucleus, and the restriction of space. Therefore, the imperfect spherulites and many microcrystals were formed for the restriction in the space. In the PET/MMT nanocomposites, the increase of the number of microcrystals and the decrease of the volume of the microcrystal augmented the interfacial area between crystals. As we know, SSP could only take place in an amorphous region[19]. The increase of the interfacial area contributed to the polycondensation of PET and diffusion of by-products. Therefore, the SSP of PET/MMT was more efficient than that of pure PET.

Figure 4 shows the WAXD patterns of two samples after 20 h SSP. It can be seen in Figure 4 that the area surrounded by the WAXD curve of pure PET was larger than that of PET/MMT after 20 h SSP, which showed that the crystallinity of pure PET was higher

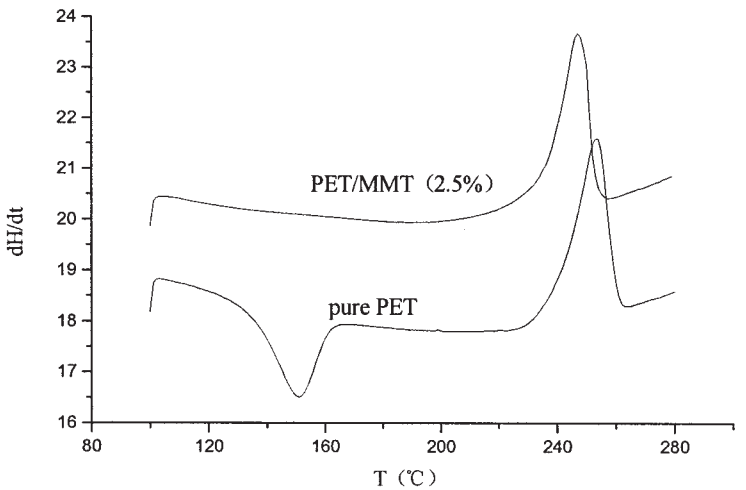

Figure 5 DSC heating curves of pure PET and PET/MMT (2.5%).

TABLE II
The DSC Thermodynamics Parameters

	Time of SSP (h)	T_m (°C)	Heat of melting ΔH (J/g)	T_c (°C)
Pure PET	0	252.07	45.68	185.72
	4	253.24	42.45	187.57
	10	253.39	40.56	191.70
	20	253.65	34.25	194.09
PET/MMT (2.5%)	0	241.32	42.57	200.69
	4	242.17	39.19	201.20
	10	242.28	37.44	204.28
	20	243.09	24.41	206.15

than that of the PET/MMT nanocomposites. This could be further proven by the DSC measurements as discussed in the following sections.

The DSC heating curves of pure PET and PET/MMT (2.5%) are presented in Figure 5. A heat-up crystallization for pure PET was indicated at 150°C, when crystallization occurred. The area of the heat-up crystallization peak (ΔH = -21.573 J/g) was smaller than that of the melting peak (ΔH = 42.66 J/g) on the curve of pure PET. The results showed that most of the pure PET molecular chains were frozen to the amorphous phase at such a cooling rate; in the heating process at the speed of 10°C/min, the PET molecular chains ranked regularly again to form the crystalline region, since they were still active when the temperature was above the glass transition temperature. So a heat-up crystallization peak occurred on the DSC curve of pure PET. However, there was no heat-up crystallization peak on the DSC curve of PET/MMT, which indicated that the PET molecular chains were active enough to freeze themselves to the crystalline phase at a rate of 160°C/min in the cooling process. This phenomenon could be considered evidence to prove that MMT accelerated the crystallization of PET.

The DSC thermodynamic parameters of pure PET and PET/MMT samples with various SSP time are given in Table II. It was noted that the melting temperature (T_m) of all samples increased a little and the crystallization temperature (T_c) increased greatly while the heat of melting decreased as the time of SSP was prolonged. The results indicated the enhancement of molecular weight, the elongation of molecular chains, and the decline of the activity of the segment with the overtime of SSP. It was also noted that the original crystallization temperature of PET/MMT (200.69°C) was higher than that of pure PET (185.72°C). This might be due to the strong interaction between the nanosized MMT layers and PET[20], which restricted the motions of PET molecular chains.

The heat of the crystalline melting was the measurement of the crystallinity. Figure 6 shows the plot of the heat of crystalline melting with various SSP times. From Figure 6, it can be seen that the crystallility of PET/MMT was rather lower than that of pure PET during the SSP process.

CONCLUSION

MMT nanomaterials had a distinct positive impact on the SSP rate of PET. This could greatly enhance the rate of SSP of PET. This enhancement might be attributed to the nucleation of MMT nanomaterials for PET crystallization, which resulted in more crystal nucleus growing. At the same time, the strong interaction between PET and MMT restricted the motions of PET segment to some extent, which prohibited the growth of PET crystalline structure and the crystallization rate of PET. This led to more amorphous regions both on the surfaces of crystals and between crystals, which further benefitted the polycondensation of PET and diffusion of by-products.

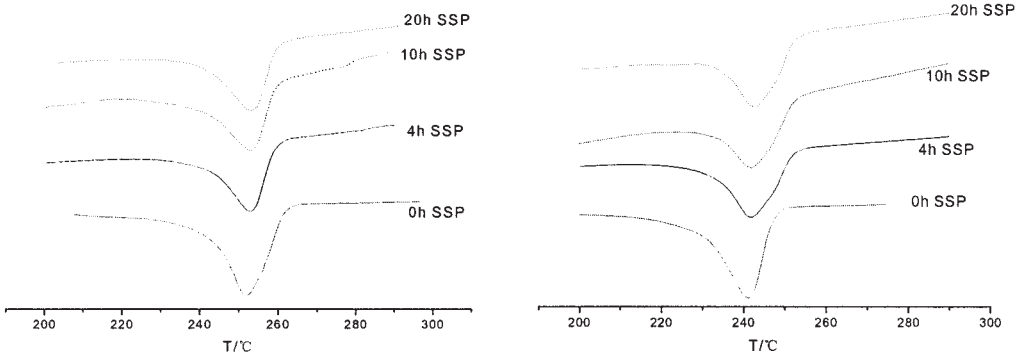

(a) Pure PET (b) PET/MMT(2.5%)

Figure 6 DSC curves of pure PET and PET/MMT (2.5%) with various SSP time.

References

1. Bamford, C. H.; Wayne, R. P. Polymer 1969, 10, 661.
2. Chen, S.-A.; Chen, F.-L. Polym Sci A Polym Chem 1987, 25, 533.
3. Devoltta, I.; Mashelkar, R. A. Chem Eng Sci 1993, 48, 1859.
4. Ravindranath, K.; Mashelkar, R. A. J Appl Polym Sci 1990, 39, 1325.
5. Chen, F. C.; Griskey, R. G.; Beyer, G. H. AIChE J 1969, 15, 680.
6. Kang, C. K. J Appl Polym Sci 1998, 68, 837.
7. Mallon, F. K.; Ray, W. H. J Appl Polym Sci 1998, 59, 1233.
8. Duh, B. J Appl Polym Sci 2001, 81, 1748.
9. Duh, B. U.S. Patent 1980, 4,205,157, May 27.
10. Kokkalos, D. E.; Bikiaris, D. N.; Karayannidis, G. P. J Appl Polym Sci 1995, 55, 787.
11. Wang, X.-Q.; Deng, D.-C. J Appl Polym Sci 2002, 83, 3133.
12. Yang, S. Synth Tech Appl 1997, 12(2), 1.
13. Tang, Z. J Appl Polym Sci 1995, 57, 473.
14. Tan, S. J Polym Sci B Polym Phys 2000, 38, 53.
15. Fann, D.-M. Polym Eng Sci 1998; 38(2), 265.
16. Jinlong, X.; Bogeng, L. Polym Mater Sci Eng 2002, 18(6), 149.
17. Qiang, Y. J Jiangsu Inst Petrol Tech 1999, 11(1), 21.
18. Guoyao, Z. Acta Polym Sin 1999, (3), 309.
19. Wang, X.; Li, W. J Donghua Univ 2002, 28(4), 128.
20. Bai, X. J Zhengzhou Univ (Eng Sci) 2002, 23(3), 91.